

Ion Storage Bias and Ion Fragmentation in the Ion Funnel Trap of a Hybrid Ion Mobility Spectrometer/Quadrupole Time-of-Flight Mass Spectrometer

GUO Zhi-da^{1,2,3}, GU Xi-xuan^{1,2,4}, WU Kai-qun^{1,2,4}, WANG Chen-lu^{1,2,4}, LI Jun-hui^{1,2,4},
YU Jian-cheng^{1,2,3}, TANG Ke-qi^{1,2,4}

(1. Zhejiang Engineering Research Center of Advanced Mass Spectrometry and Clinical Application, Institute of Mass Spectrometry, Ningbo University, Ningbo 315211, China; 2. Zhenhai Institute of Mass Spectrometry, Ningbo 315211, China; 3. Faculty of Electrical Engineering and Computer Science, Ningbo University, Ningbo 315211, China; 4. School of Material Science and Chemical Engineering, Ningbo University, Ningbo 315211, China)

Abstract: In this study, a detailed experimental characterization of the relative ion abundance bias and the ion fragmentation in an ion funnel trap were reported by using both cytochrome C and ubiquitin samples in a tandem ion funnel hybrid ion mobility spectrometer/quadrupole time-of-flight mass spectrometer (IMS/QTOF MS). Specifically, signals of multiple interfering ions appeared in the MS spectra acquired at a relatively short ion filling time of the ion funnel trap for both selected protein samples, while they were absent at longer ion filling time. Further MS/MS studies confirmed that these interfering ions are derived from the fragmentation of the protein ions occurring before the IMS drift tube. The possible reasons for the ion fragmentation, including the ion fragmentation at the exit of the inlet capillary and the radio frequency (RF) heating in two ion funnels, were systematically studied. By carefully adjusting the voltages on each relevant component, the experimental results demonstrated that the ion fragmentation indeed occurs in the ion funnel trap due to excessive RF heating when the RF voltage was higher than 130 V. Therefore, it is extremely important to set the reasonable operation conditions for the ion funnel trap to avoid both ion fragmentation and ion storage bias in IMS/QTOF MS.

Key words: ion mobility spectrometry-mass spectrometry (IMS-MS); ion funnel; radio frequency (RF) voltage; ion fragmentation

CLC number: O657.63

Document code: A

Article ID: 1004-2997(2026)02-0157-09

DOI: [10.7538/zpxb.2025.0054](https://doi.org/10.7538/zpxb.2025.0054)

CSTR: [32365.14.zpxb.2025.0054](https://cstr.cn/32365.14.zpxb.2025.0054)

离子迁移质谱联用仪捕集离子漏斗中的离子 存储偏差及离子裂解效应

郭志达^{1,2,3}, 顾希焯^{1,2,4}, 吴凯群^{1,2,4}, 王陈璐^{1,2,4}, 李俊晖^{1,2,4},
俞建成^{1,2,3}, 唐科奇^{1,2,4}

(1. 宁波大学质谱技术与应用研究院, 高端质谱技术和临床应用浙江省工程研究中心, 浙江 宁波 315211;

2. 宁波镇海质谱技术研究院, 浙江 宁波 315211; 3. 宁波大学信息科学与工程学院, 浙江 宁波 315211;

4. 宁波大学材料科学与化学工程学院, 浙江 宁波 315211)

摘要: 采用串联离子漏斗的离子迁移谱/四极杆飞行时间质谱(IMS/QTOF MS)分析细胞色素 C 和泛素样品, 研究捕集离子漏斗中的离子相对丰度偏差和离子碎裂效应。对于蛋白质样品, 在捕集离子漏斗离子填充时间相对较短的情况下, 采集的质谱图中会出现多个干扰离子信号; 而在较长的离子填充条件下, 未观察到干扰离子信号。进一步通过二级质谱碎片分析证实, 这些干扰离子是由离子迁移谱漂移管前的蛋白质离子断裂效应产生的。此外, 还系统研究了可能导致离子裂解的原因, 包括质谱离子入口处的源内裂解电压及 2 个离子漏斗中的射频加热。通过优化每个相关组件上的电压, 发现当捕集离子漏斗的射频电压高于 130 V 时, 过度射频加热会在捕集离子漏斗内发生离子裂解。因此, 为捕集离子漏斗设置合理的操作条件, 对于避免离子裂解和离子存储偏差具有重要意义。

关键词: 离子迁移质谱(IMS-MS); 离子漏斗; 射频电压; 离子裂解

The function and bioactivity of proteins are primarily associated with their molecular composition and three-dimensional (3D) structure^[1-2]. Proteins with abnormal molecular composition or 3D structure are the main causes of many malignant diseases, such as Alzheimer's disease^[3-4], Parkinson's disease^[5-6] and cancer^[7-8]. Accurate determination of both molecular composition and 3D structure of intact proteins in their native environment is one of the research hotspots in current proteomics. Electrospray ionization-ion mobility spectrometry-mass spectrometry (ESI-IMS-MS) is a widely utilized technique for converting molecules into intact molecular ions^[9], separating isomeric ions, and measuring both the mass-to-charge ratio (m/z) and the cross-section area of the molecular ions^[10-11]. The measured m/z and cross-section area of ions can be further used to simultaneously determine the original molecular composition and structure of the molecular ions^[12-13]. Due to its high-throughput, high-sensitivity and rapid detection speed, ESI-IMS-MS has increasingly become an important technique for proteomics research^[14-16].

At present, multiple ESI-IMS-MS techniques have been developed, mainly including ESI-drift tube IMS (DTIMS)-MS, ESI-trapped IMS (TIMS)-MS, ESI-traveling wave IMS (TWIMS)-MS, ESI-cyclic IMS (CIMS)-MS and ESI-high-field asymmetric waveform IMS (FAIMS)-MS^[17-18]. Among these techniques, ESI-DTIMS-MS is the one allowing a simple calculation to determine the cross-section area of the ions *via* the Mason-Schamp equation, based on the measured drift time of ions in DTIMS^[12-13]. Accurate structure characterization of isomeric molecules can be further achieved by combining the measured cross-section area of the ions with a rigorous molecular dynamic simulation^[12]. This makes ESI-DTIMS-MS a unique technique for the structural and compositional characterization of protein molecules.

The current leading commercial ESI-DTIMS-MS instrument is the Agilent 6560 IMS-QTOF (quadrupole time-of-flight) MS. As shown in Fig.S1 (Please check out website at <https://zpxb.xml-journal.net/>), a regular high-pressure ion funnel and an ion funnel trap were used in tandem as the ESI-

IMS interface of the instrument to achieve high-sensitivity^[11]. With the use of the high-pressure ion funnel, operating in the pressure range of 666.6-800.0 Pa, the dispersed ion beam carried by the expanding gas jet at the exit of the inlet capillary would be radially captured at the large diameter (~ 25 mm) inlet of the ion funnel by the radio frequency (RF) field applied to the ion funnel^[19-20]. A direct current (DC) electric field established along the axial direction of the ion funnel effectively drives all the ions toward the funnel exit^[21-22]. Meanwhile, the ion beam entering the ion funnel would be gradually focused to a small diameter by the RF field as the inner diameter of ring electrode for the ion funnel is gradually reduced to about 2 mm at the funnel exit^[21-22]. High ion transmission efficiency was thus achieved between the high-pressure ion funnel and the second stage ion funnel trap, operating at a lower gas pressure of ~ 533.3 Pa. Unlike the high-pressure ion funnel, a special hourglass shaped geometry was used for the ion funnel trap to allow ion accumulation between each IMS measurement and achieve high duty cycle of the instrument^[23-24]. According to the experimental performance evaluation, an order of sensitivity improvement can be achieved with such instrument design^[25].

Although the sensitivity of ESI-IMS-MS can be dramatically improved by using the tandem ion funnel interface, an ion storage bias associated with ion structure in the ion funnel trap was also discovered in our previous studies^[11,13], which can significantly influence the accuracy of the structural characterization for isomeric ions. In this study, another ion storage bias would cause the changes in the relative abundances of ions with different m/z under varying ion filling times of ion funnel trap was further found. In addition, an unknown ion fragmentation of protein ion before the IMS drift tube was also observed. To identify the possible reasons for the ion fragmentation, the effects of the related instrument operating parameters, including the fragmentor voltage and the RF voltages of the two ion funnels, on the ion fragmentation were systematically investigated.

1 Experimental Section

1.1 Sample Preparation

Cytochrome C ($\sim 12\ 230$ u) was purchased from Beijing Biosynthesis Biotechnology Co. Ltd (Beijing, China). Ubiquitin (*N*-terminal histidine tagged, $\sim 10\ 030$ u) was purchased from Sigma-Aldrich Co. LLC (Darmstadt, Germany). HPLC grade methanol and acetic acid were purchased from Fisher Scientific Inc. (Pittsburgh, PA, USA). Deionized water was generated using a Milli-Q water purification system from Millipore (Billerica, MA, USA).

A mixture of deionized water/methanol/acetic acid (50:50:1, *V/V/V*) was used as the solvent for all the sample solutions in this study. The stock solutions of ubiquitin and cytochrome C at a concentrations of 1 mmol/L were firstly prepared by directly dissolving the samples in deionized water. Subsequently, both the 1 mmol/L stock solutions of ubiquitin and cytochrome C were further diluted to 10 $\mu\text{mol/L}$ with the solvent mixture, respectively, prior to ESI-IMS-MS analysis.

1.2 Instruments and Experimental Conditions

Both the 10 $\mu\text{mol/L}$ ubiquitin and cytochrome C solutions were analyzed on an Agilent 6560 IMS-QTOF MS instrument. All the analyte ions were produced by a nano-ESI source operated under positive ion mode. The flow rate and the capillary voltage of the nano-ESI source were set at 0.3 $\mu\text{L/min}$ and 3.5 kV, respectively. The temperature and the flow rate of the drying gas for IMS-QTOF MS were set at 45 $^{\circ}\text{C}$ and 4.5 L/min, respectively. The N_2 buffer gas pressure in the ion funnel trap and IMS drift tube were controlled at 513.3, 533.3 Pa and 4.00 Torr, respectively. The maximum drift time of IMS (t_d) was set at 70 ms. The ion filling time (t_f) of the ion funnel trap was varied in the range of 15-65 ms with an increment of 10 ms, and the trap release time was set at 100 μs . The default RF voltages for both the regular high-pressure ion funnel (V_R) and the ion funnel trap (V_T) were set at 150 $V_{\text{p-p}}$. The default fragmentor voltage (V_F) was set at 300 V. The other parameters of the IMS-QTOF MS platform were kept at the default values.

2 Results and Discussion

The 10 $\mu\text{mol/L}$ cytochrome C sample was first analyzed using IMS-QTOF MS at different t_f ranging from 15 ms to 65 ms, with fixed $V_R=V_T=150$ V and $t_d=70$ ms. The MS spectra of the cytochrome C sample acquired at $t_f=65$ ms and 15 ms are shown in Fig.1, whereas those acquired at $t_f=25, 35, 45, 55$ ms are shown in Fig.S2. The cytochrome C ions with charge states distributed in the range of +8 to +19 can be clearly observed in Fig.1 and Fig.S2. The relative abundances (R_a) of cytochrome C ions with different charge states are essentially the same in the MS spectra acquired at different t_f . However, while a clean spectrum of cytochrome C ions with various

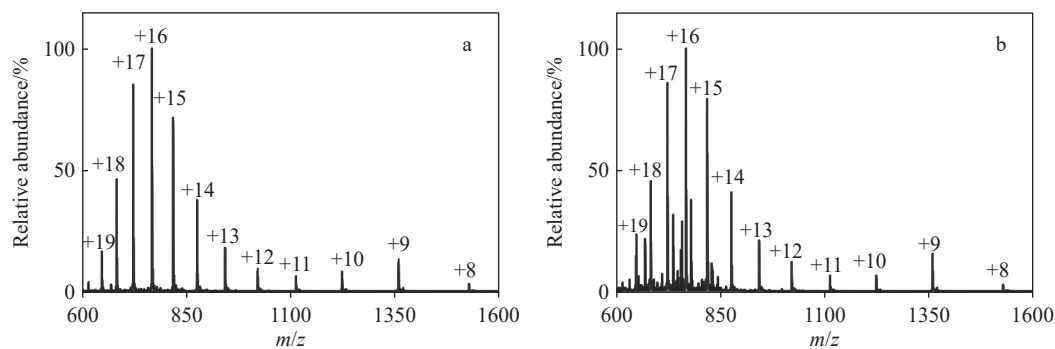


Fig. 1 MS spectra of cytochrome C ions acquired at $t_f=65$ ms (a) and 15 ms (b), with $V_R=V_T=150$ V and $t_d=70$ ms

In our previous studies, an ion storage bias was identified in the ion funnel trap of the Agilent 6560 IMS-QTOF MS^[11,13]. Specifically, the number of ions stored in the ion funnel trap initially increases with increasing t_f and reaches a maximum value at a specific t_f , indicating that the ion funnel trap is fully filled. When the number of ions stored in ion funnel trap exceeds a specific value (lower than the maximum number that can be stored in the ion funnel trap), an unavoidable ion storage bias would occur and the conformers with extended structures would be filled less efficiently if further ion filling is allowed^[11]. Accordingly, a significant structural bias in the acquired IMS spectra would be observed. The experimental results showed in Fig.1, Fig.S2 and Fig.S3 indicated that besides the ion structural bias, a new bias exists as the interfering peaks are only clearly detected at shorter filling time.

charge states, as shown in Fig.1a, can be obtained at $t_f=65$ ms, some unknown interfering peaks can be clearly observed in the one acquired at $t_f=15$ ms as shown in Fig.1b. Furthermore, according to Fig.1 and Fig.S2, it also can be found that the R_a of these interfering peaks gradually increases with decreasing t_f . Fig.S3 further showed the MS spectra of 10 $\mu\text{mol/L}$ ubiquitin sample, which were also acquired at different t_f (15-65 ms) with fixed $V_R=V_T=150$ V and $t_d=70$ ms. Same phenomenon occurred. In the ubiquitin spectra, while the R_a of ubiquitin ions with charge state +9 to +15 are basically the same under different t_f , unknown interfering peaks appear at smaller t_f , and their R_a increases significantly as t_f decreases.

To understand the phenomenon observed in Fig.1, Fig.S2 and Fig.S3, five interfering ions (named as ions C1 to C5) in the MS spectra of cytochrome C and four interfering ions (named as ions U1 to U4) in the MS spectra of ubiquitin, whose R_a clearly changed at different t_f were selected for further investigation, respectively. The m/z and the charge state of each selected interfering ions are listed in Table 1, and the corresponding R_a of these nine ions under different t_f conditions are shown in Fig.2. As shown in Fig.2, the R_a values for all these ions decrease continuously decreasing t_f at $V_T=150$ V. Especially, the R_a for U3 ions decreases from $\sim 91.2\%$ to $\sim 1.6\%$ as t_f increases from 15 ms to 65 ms. The results shown in Fig.2 also indicated that this bias exists in the broad range of t_f and is somewhat difficult to be eliminated as compared to the structural bias in ion funnel trap, as the structural

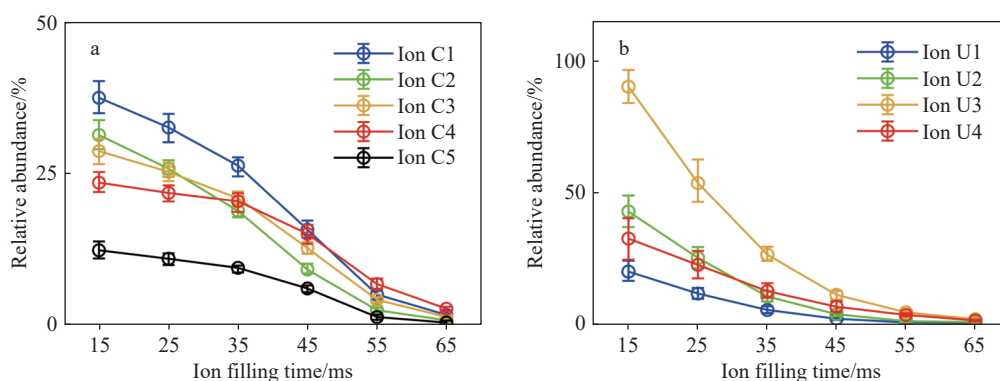


Fig. 2 Relative abundances of interfering ions acquired at different t_f in the MS spectra of cytochrome (a) and ubiquitin (b)

Table 1 Information on interfering ions observed in the MS spectra of cytochrome C and ubiquitin samples

Sample	Ion	m/z	Charge state	Molecular mass
Cytochrome C	C1	777.6	+6	4659.6
	C2	734.2	+6	4399.2
	C3	755.7	+6	4528.2
	C4	666.6	+7	4659.2
	C5	827.4	+9	7437.6
Ubiquitin	U1	875.9	+4	3499.6
	U2	817.3	+8	6530.4
	U3	726.6	+9	6530.4
	U4	654.0	+10	6530.4

bias in ion funnel trap can be eliminated by setting $t_f < 28$ ms and $V_T \leq 160$ V^[11].

From Table 1, the four interfering ions appeared in the ubiquitin spectra can be simply deconvoluted, based on their charge states, into two different molecular masses of 3 499.6 and 6 530.4. The sum of these two molecular masses exactly equals the molecular mass of ubiquitin (10 030.0), which strongly suggested that the ions U1 to ion U4 might be the fragments of the ubiquitin ions. As the R_a of these fragment ions would vary with the change of t_f and be apparently eliminated from the spectra at longer t_f , as shown in Fig.S3a and Fig.S3b with $t_f=65$ ms and 55 ms, respectively. Consequently, these fragment ions must be generated prior to the IMS drift tube according to the schematics of the Agilent 6560 IMS-QTOF MS (Fig.S1). However, the identities for the interfering ions appeared in the

cytochrome C mass spectra are a bit more difficult to determine as the C1 to C5 ions can be deconvoluted into four different molecular masses, which also disappear at a longer ion filling time of $t_f=65$ ms (Fig.1a). To verify whether ions C1 to C5 are also the fragments of cytochrome C ions, MS/MS spectrum was further acquired at collision energy of 10 V in the instrument's collision cell. This experiment was conducted under ion funnel operating conditions ($V_R=V_T=150$ V and $t_f=65$ ms) that ensures no interfering ions enter the collision cell. As shown in Fig.3, the signal of ions C1 to C5 can all be clearly observed in the acquired MS/MS spectrum based on their specific m/z . This convincingly confirmed that ions C1 to C5 are indeed fragments of cytochrome C ions as well.

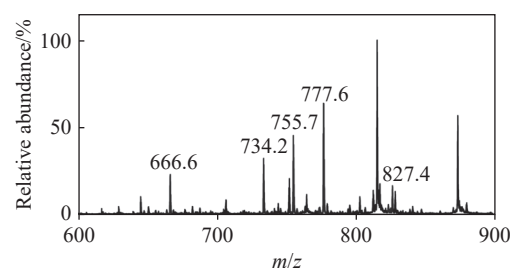


Fig. 3 MS/MS spectrum of the 10 $\mu\text{mol/L}$ cytochrome C solution acquired at a collision energy of 20 V, with $t_f=65$ ms, $V_R=V_T=150$ V and $t_d=70$ ms

According to our previous study, it is important to set $V_T \leq 160$ V and $t_f < 28$ ms in order to eliminate the structural bias in ion funnel trap^[11]. However, as shown in Fig.1, Fig.S2 and Fig.S3, protein fragment ions can be clearly observed in the MS spectra under

these operating conditions. Based on the specific design of the Agilent IMS-QTOF MS instrument, three components are located upstream of the IMS drift tube, including the inlet capillary, the regular high-pressure ion funnel, and the ion funnel trap. The possible parameters that can cause ion fragmentation include the fragmentor voltage (ion/background gas collision associated fragmentation) and the RF voltages of both the regular high-pressure ion funnel and the ion funnel trap (RF heating associated ion fragmentation)^[26]. To eliminate ion fragmentation,

the effect of these voltages on the ion fragmentation was experimentally evaluated. The fragmentor voltage was first tested, and the MS spectra of the 10 $\mu\text{mol/L}$ cytochrome C and ubiquitin samples were acquired at $V_F=250, 300$ and 350 V, respectively, with fixed $t_f=15$ ms, $V_R=V_T=150$ V and $t_d=70$ ms. As shown in Fig.4 and Fig.S4, the R_a values for all the cytochrome C, ubiquitin and the protein fragment ions remain the same under different V_F , which confirms that the fragmentation of protein ions is not caused by the fragmentor voltage.

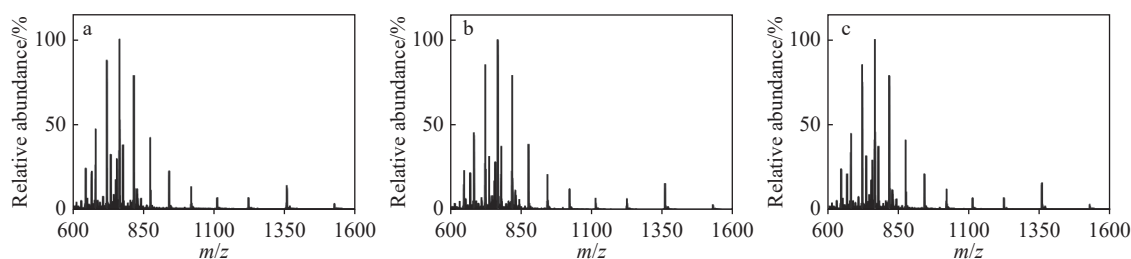


Fig. 4 MS spectra of the 10 $\mu\text{mol/L}$ cytochrome C sample acquired at $V_F=250$ V (a), 300 V (b) and 350 V (c), with $t_f=15$ ms, $V_R=V_T=150$ V and $t_d=70$ ms

To further test the possibility of ion fragmentation caused by RF heating in the two ion funnels, the MS spectra of ubiquitin and cytochrome C samples were acquired at different V_R and V_T . Fig.5 and Fig.S5 show the MS spectra of the 10 $\mu\text{mol/L}$ cytochrome C and ubiquitin solutions acquired at $V_R=110, 130$ and 150 V, respectively, with fixed $t_f=15$ ms, $V_T=150$ V and $t_d=70$ ms. As shown in Fig.5 and Fig.S5, the R_a values for all cytochrome C, ubiquitin and the protein fragment ions also remain the same under different V_R , which indicated that the fragmentation of protein ions is not caused by the RF heating in the regular high-pressure ion funnel.

Fig.S4, Fig.5 and Fig.S5 demonstrated that the RF heating in the ion funnel trap is the only possible reason to cause the fragmentation of protein ions. Therefore, the MS spectra of ubiquitin and cytochrome C samples were further acquired at different V_T . Fig.6 and Fig.S6 showed the MS spectra of the 10 $\mu\text{mol/L}$ cytochrome C and ubiquitin solutions acquired at $V_T=130, 140, 150$ and 160 V, respectively, with fixed $t_f=15$ ms, $V_R=150$ V and $t_d=70$ ms. The results in Fig.6 and Fig.S6 indicated that the R_a values of cytochrome C and ubiquitin ions with different charge states remain essentially the same under different V_T values, while the R_a values of all cytochrome C and ubiquitin fragment ions

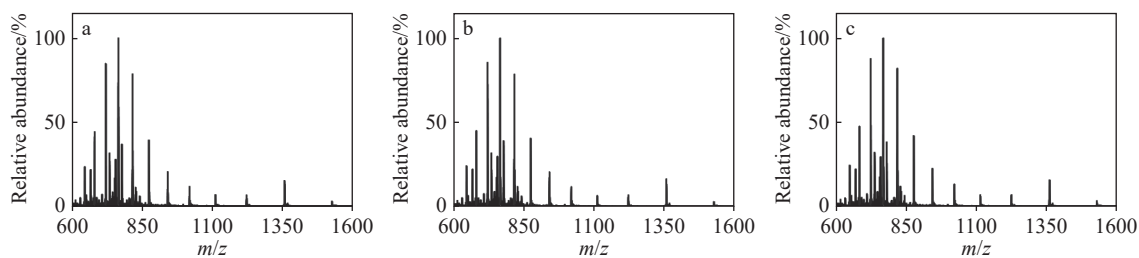


Fig. 5 MS spectra of the 10 $\mu\text{mol/L}$ cytochrome C solution acquired at $V_R=110$ V (a), 130 V (b) and 150 V (c), with $t_f=15$ ms, $V_T=150$ V and $t_d=70$ ms

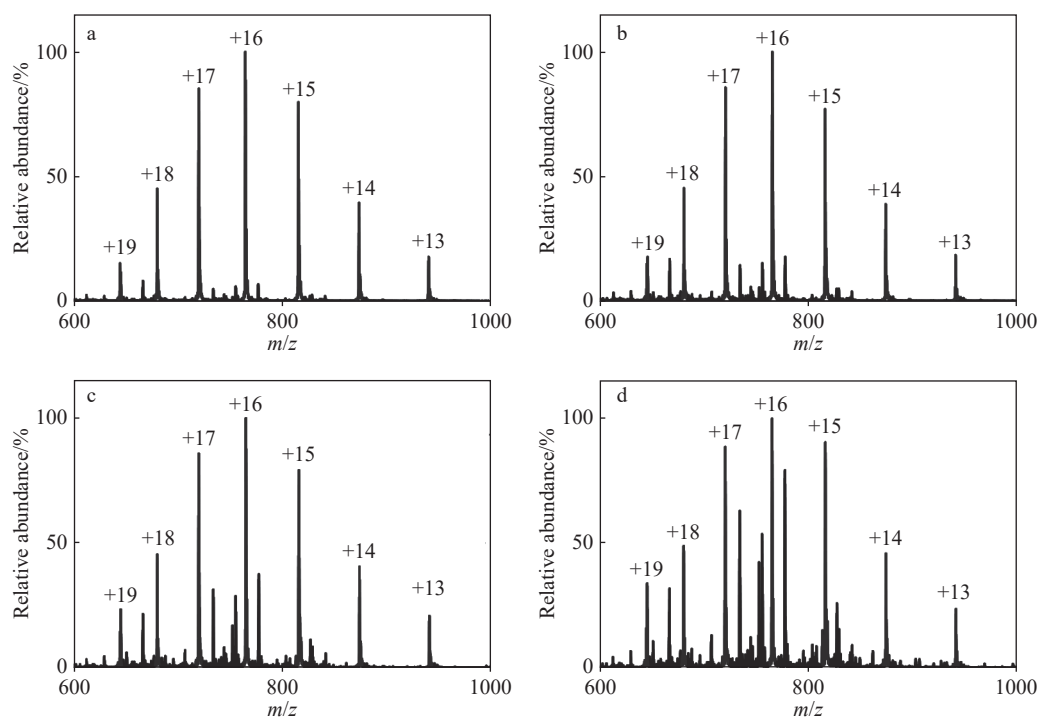


Fig. 6 MS spectra of the 10 $\mu\text{mol/L}$ cytochrome C solution acquired at $V_T=130$ V (a), 140 V (b), 150 V (c) and 160 V (d), with $t_r=15$ ms, $V_R=150$ V and $t_d=70$ ms

increase continuously with the increasing V_T . By varying V_T from 130 V to 160 V, an order of magnitude increase of the R_a values by all the cytochrome C fragment ions were observed, as shown in Fig.6. Similarly, as shown in Fig.S6, the R_a values of all ubiquitin fragment ions also increase by an order of magnitude as V_T increases from 130 V to 160 V. It also can be observed in Fig.6a, the signals of cytochrome C fragment ions are already negligible at $V_T=130$ V. In Fig.S6a, the signals of ubiquitin fragment ions are also essentially negligible in the MS spectrum acquired at $V_T=130$ V. These experimental results clearly proved that protein ion fragmentation indeed occurred in the ion funnel trap due to the RF heating, as the R_a of all protein fragment ions increase significantly with the increase of V_T . The reason for the protein ion fragmentation occurred only in the ion funnel trap may be due to the different operating gas pressure and RF heating time compared with those in the regular high-pressure ion funnel. The gas pressure in the ion funnel trap (513.3 Pa) is lower than that in the regular high-pressure ion funnel ($\sim 666.6\text{--}800.0$ Pa),

which causes the increase of the collision energy between protein ions and background neutral gas molecules. More importantly, the protein ions would be stored in the ion funnel trap for 70 ms (far longer than the storage time of ion in the regular high-pressure ion funnel), which further increases the RF heating time. The increasing internal energy of ion can be calculated as

$$Q = U^2/R \cdot t = m \cdot c \cdot (T_{\text{fin}} - T_{\text{ini}})$$

where U is the amplitude of RF voltage, R is the resistance of ion funnel, t is the storage time of ion in the ion funnel, m is the mass of ion, c is the specific heat capacity of ion, T_{fin} is the final temperature of ion, and T_{ini} is the initial temperature of ion. This equation indicated that the increase of the internal energy for ion caused by RF heating is directly related to the RF voltage and the ion storage time in the ion funnel. Higher RF voltage and longer ion storage time lead to a significant increase in the internal energy of ions. When the internal energy of ions exceeds a specific threshold, protein ion fragmentation occurs. Overall, according to the experimental results shown in Fig.6, Fig.S6 and our

previous study^[11], it is possible to eliminate both ion fragmentation and ion structural bias in the ion funnel trap of Agilent 6560 IMS-QTOF MS by setting $V_T \leq 130$ V and $t_f \leq 28$ ms.

A DC electric field was also established in the axial direction of the ion funnel, which effectively pushes all the ions toward the exit of the ion funnel. This DC voltage may also affect ion fragmentation in the ion funnel. Therefore, the MS spectra of the 10 $\mu\text{mol/L}$ cytochrome C solution were further acquired at different DC voltages of the regular high-pressure ion funnel (V_{DR}) and the ion funnel trap (V_{DT}), respectively, with $V_R=150$ V and $V_T=130$ V. As shown in Fig.S7, the MS spectra of cytochrome C sample were first acquired at $V_{DR}=120$ V, 150 V (the default value) and 180 V, with $V_{DT}=150$ V (the default value). The MS spectra acquired at different V_{DR} are essentially the same, and the signals of cytochrome C fragment ions are basically negligible. The similar experimental results were also observed in the MS spectra of cytochrome C sample acquired at $V_{DT}=120$ V, 150 V (the default value) and 180 V as shown in Fig.S8, with $V_{DR}=150$ V. These experimental results clearly prove that the DC voltage of two ion funnels plays a negligible role in the ion fragmentation in the ion funnel.

3 Conclusions

In this study, the relative ion abundance bias in the ion funnel trap was first systematically explored using cytochrome C and ubiquitin samples. It was observed that the relative abundance of multiple interfering ions increases continuously by decreasing ion filling time of ion funnel trap in the acquired MS spectra of two protein samples. This results in multiple interfering ions that cannot be observed in the MS spectra acquired at longer t_f while can be clearly observed in the ones acquired at shorter t_f . Interestingly, further studies proved that these interfering ions are actually fragments of the analyzed protein ions, generated by RF heating in the ion funnel trap when operated with $V_T > 130$ V. Therefore, according to the experimental results

shown in this study and our previous study, to avoid both ion fragmentation and structural bias in the ion funnel trap during the IMS-MS analysis of intact protein, it is necessary to set $V_T \leq 130$ V and $t_f < 28$ ms.

References:

- [1] CLEMMER D E, RUSSELL D H, WILLIAMS E R. Characterizing the conformationome: toward a structural understanding of the proteome[J]. *Accounts of Chemical Research*, 2017, 50(3): 556-560.
- [2] HAN L, RUOTOLO B T. Ion mobility-mass spectrometry differentiates protein quaternary structures formed in solution and in electrospray droplets[J]. *Analytical Chemistry*, 2015, 87(13): 6 808-6 813.
- [3] KIRKITADZE M D, BITAN G, TEPLow D B. Paradigm shifts in Alzheimer's disease and other neurodegenerative disorders: the emerging role of oligomeric assemblies[J]. *Journal of Neuroscience Research*, 2002, 69(5): 567-577.
- [4] RAHMAN M M, LENDEL C. Extracellular protein components of amyloid plaques and their roles in Alzheimer's disease pathology[J]. *Molecular Neurodegeneration*, 2021, 16(1): 59.
- [5] BI M, DU X, JIAO Q, CHEN X, JIANG H. Expanding the role of proteasome homeostasis in Parkinson's disease: beyond protein breakdown[J]. *Cell Death & Disease*, 2021, 12(2): 154.
- [6] PICCA A, GUERRA F, CALVANI R, ROMANO R, COELHO-JÚNIOR H J, BUCCI C, MARZETTI E. Mitochondrial dysfunction, protein misfolding and neuroinflammation in Parkinson's disease: roads to biomarker discovery[J]. *Biomolecules*, 2021, 11(10): 1 508.
- [7] MERENBAKH-LAMIN K, BEN-BARUCH N, YEHESEKEL A, DVIR A, SOUSSAN-GUTMAN L, JESELSOHN R, YELENSKY R, BROWN M, MILLER V A, SARID D, RIZEL S, KLEIN B, RUBINEK T, WOLF I. D538G mutation in estrogen receptor- α : a novel mechanism for acquired endocrine resistance in breast cancer[J]. *Cancer Research*, 2013, 73(23): 6 856-6 864.
- [8] SRIVASTAVA S, JAYASWAL N, KUMAR S, SHARMA P K, BEHL T, KHALID A, MOHAN S, NAJMI A, ZOGHEBI K, ALHAZMI H A. Unveiling the potential of proteomic and genetic signatures for precision therapeutics in lung cancer management[J]. *Cellular Signalling*, 2024, 113: 110 932.

- [9] BANERJEE S, MAZUMDAR S. Electrospray ionization mass spectrometry: a technique to access the information beyond the molecular weight of the analyte[J]. *International Journal of Analytical Chemistry*, 2012, 2012(1): 282-574.
- [10] MYUNG S, WISEMAN J M, VALENTINE S J, TAKÁTS Z, COOKS R G, CLEMMER D E. Coupling desorption electrospray ionization with ion mobility/mass spectrometry for analysis of protein structure: evidence for desorption of folded and denatured states[J]. *The Journal of Physical Chemistry B*, 2006, 110(10): 5 045-5 051.
- [11] LI J, LIU R, GAO W, YU J, TANG K. Ion storage biases in the ion funnel trap of a Hybrid ion mobility spectrometer/time of flight mass spectrometer[J]. *Talanta*, 2023, 260: 124-621.
- [12] TANG K, LI F, SHVARTSBERG A A, STRITTMATTER E F, SMITH R D. Two-dimensional gas-phase separations coupled to mass spectrometry for analysis of complex mixtures[J]. *Analytical Chemistry*, 2005, 77(19): 6 381-6 388.
- [13] LI J, LI L, GAO W, SHI S, YU J, TANG K. Two-dimensional FAIMS-IMS characterization of peptide conformers with resolution exceeding 1000[J]. *Analytical Chemistry*, 2022, 94(16): 6 363-6 370.
- [14] McLEAN J A, RUOTOLO B T, GILLIG K J, RUSSELL D H. Ion mobility-mass spectrometry: a new paradigm for proteomics[J]. *International Journal of Mass Spectrometry*, 2005, 240(3): 301-315.
- [15] LOKHNAUTH J K, SNOW N H. Solid phase microextraction coupled with ion mobility spectrometry for the analysis of ephedrine in urine[J]. *Journal of Separation Science*, 2005, 28(7): 612-618.
- [16] GLISH G L, VACHET R W. The basics of mass spectrometry in the twenty-first century[J]. *Nature Reviews Drug Discovery*, 2003, 2(2): 140-150.
- [17] CUMERAS R, FIGUERAS E, DAVIS C E, BAUMBACH J I, GRÀCIA I. Review on ion mobility spectrometry. Part 1: current instrumentation[J]. *The Analyst*, 2015, 140(5): 1 376-1 390.
- [18] CUMERAS R, FIGUERAS E, DAVIS C E, BAUMBACH J I, GRÀCIA I. Review on ion mobility spectrometry. Part 2: hyphenated methods and effects of experimental parameters[J]. *The Analyst*, 2015, 140(5): 1 391-1 410.
- [19] SHAFFER S A, TANG K, ANDERSON G A, PRIOR D C, UDSETH H R, SMITH R D. A novel ion funnel for focusing ions at elevated pressure using electrospray ionization mass spectrometry[J]. *Rapid Communications in Mass Spectrometry*, 1997, 11(16): 1 813-1 817.
- [20] SHAFFER S A, PRIOR D C, ANDERSON G A, UDSETH H R, SMITH R D. An ion funnel interface for improved ion focusing and sensitivity using electrospray ionization mass spectrometry[J]. *Analytical Chemistry*, 1998, 70(19): 4 111-4 119.
- [21] KIM T, TOLMACHEV A V, HARKEWICZ R, PRIOR D C, ANDERSON G, UDSETH H R, SMITH R D. Design and implementation of a new electrodynamic ion funnel[J]. *Analytical Chemistry*, 2000, 72(10): 2 247-2 255.
- [22] BELOV M E, CLOWERS B H, PRIOR D C, DANIELSON W F, LIYU A V, PETRITIS B O, SMITH R D. Dynamically multiplexed ion mobility time-of-flight mass spectrometry[J]. *Analytical Chemistry*, 2008, 80(15): 5 873-5 883.
- [23] IBRAHIM Y, BELOV M E, TOLMACHEV A V, PRIOR D C, SMITH R D. Ion funnel trap interface for orthogonal time-of-flight mass spectrometry[J]. *Analytical Chemistry*, 2007, 79(20): 7 845-7 852.
- [24] CLOWERS B H, IBRAHIM Y M, PRIOR D C, DANIELSON W F, BELOV M E, SMITH R D. Enhanced ion utilization efficiency using an electrodynamic ion funnel trap as an injection mechanism for ion mobility spectrometry[J]. *Analytical Chemistry*, 2008, 80(3): 612-623.
- [25] TANG K, SHVARTSBERG A A, LEE H N, PRIOR D C, BUSCHBACH M A, LI F, TOLMACHEV A V, ANDERSON G A, SMITH R D. High-sensitivity ion mobility spectrometry/mass spectrometry using electrodynamic ion funnel interfaces[J]. *Analytical Chemistry*, 2005, 77(10): 3 330-3 339.
- [26] SHVARTSBERG A A, LI F, TANG K, SMITH R D. Distortion of ion structures by field asymmetric waveform ion mobility spectrometry[J]. *Analytical Chemistry*, 2007, 79(4): 1 523-1 528.

(Received date: 2025-05-05; Revised date: 2025-06-30)